Solitons and magnon bound states in ferromagnetic Heisenberg chains

T. Schneider
IBM Zurich Research Laboratory, 8803 Rüschlikon, Switzerland
(Received 6 March 1981; revised manuscript received 6 May 1981)

We investigate the relation between magnon, magnon bound states, and the classical soliton solutions in the isotropic, the anisotropic-exchange, and the easy-axis ferromagnetic Heisenberg chains. The Dyson-Maleev boson representation is used to study the interaction between magnons, and bound states are investigated in terms of two-spin Green's functions. For easy-axis and anisotropic-exchange magnets, a mapping to the Bose gas with attractive δ-function interactions is established, and it yields the eigenvalues of the magnon and the mth bound state in the weak-coupling and continuum limits. The classical limit of the two-spin Green's function reveals that, to leading order in temperature, the bound-state resonance and the associated effects on the two-magnon continuum survives. An important result is a T^2 dependence of the "binding" energy of the bound-state resonance. As a consequence, in a classical description the bound states enter only in order T^2. Finally, we quantize the soliton solutions according to the Bohr-Sommerfeld and de Broglie rules. This approach is found to be exact for the $s=\frac{1}{2}$ isotropic Heisenberg chain and for sufficiently small wave numbers for all s values. In the anisotropic-exchange and easy-axis models, it agrees with the results obtained from the mapping on the Bose gas, for large quantum numbers and in the easy-axis case for $s \gg \frac{1}{2}$ in addition. On this basis, we conclude that the envelope solitons considered here lead to bound-state resonances and associated effects in a classical treatment. Moreover, their semiclassical quantization gives remarkably accurate energy levels.

I. INTRODUCTION

The quantum and classical properties of ferromagnetic linear chains, including the eigenvalue spectrum, the soliton features, the dynamics and thermodynamics, are important subjects of theoretical and experimental studies.[1]

Classical results include: transfer integral calculations for thermodynamic quantities and static correlation functions,[2–6] computer simulations of dynamic properties,[6–8] exact results for the dynamics in the isotropic Heisenberg chain at low temperatures to leading order in T,[9] computer simulations of continuum models, revealing soliton characteristics,[10,11] and discovery of the exact integrability of various continuum models by means of the inverse-scattering method.[12,13]

The quantum aspects have been studied extensively since the pioneering work of Bethe in 1931 (Ref. 14) on the spin-$\frac{1}{2}$ Heisenberg chain. He classified the states in terms of magnons and magnon bound states. The lattice method developed by Baxter for the eight-vertex model, inspired by Bethe's eigenfunctions, also led to the eigenfunctions and the eigenvalue spectrum of the spin-$\frac{1}{2}$ XYZ model by Baxter,[15] Sutherland,[16] and by Johnson, Krinsky and McCoy.[17] Recently, a close connection between Baxter's technique and the quantum-mechanical extension of the inverse-scattering method has been established.[18,19]

In this paper, we make a comparative study of some classical and quantum aspects of discrete and continuum Heisenberg ferromagnetic chains. The discrete versions are defined by the Hamiltonians: isotropic Heisenberg chain (IH)

$$\mathcal{H} = -J\sum_{i=1}^{N}\vec{S}_{i+1}\cdot\vec{S}_i + h\sum_{i=1}^{N}S_i^z \;; \tag{1}$$

easy-axis Heisenberg chain (EAH)

$$\mathcal{H} = -J\sum_{i=1}^{N}\vec{S}_{i+1}\cdot\vec{S}_i - D\sum_{i=1}^{N}(S_i^z)^2 + h\sum_{i=1}^{N}S_i^z \tag{2}$$

with

$$D \geqslant 0 \;; \tag{3}$$

and anisotropic-exchange Heisenberg (AEH)

$$\mathcal{H} = -J\sum_{i=1}^{N}\left[S_{i+1}^zS_i^z + \frac{1}{g}(S_{i+1}^xS_i^x + S_{i+1}^yS_i^y)\right] + h\sum_{i=1}^{N}S_i^z \tag{4}$$

with

$$g \geqslant 1 \;. \tag{5}$$

$\vec{S}_i$ denotes the spin operator at the ith site, and a ferromagnetic coupling

$$J > 0 \tag{6}$$

is assumed.

Since the Hamiltonians given by Eqs. (1), (2), and (4) commute with the total z component of the spin

$$m_{op} = \sum_l S_l^z - S_0^z \tag{7}$$

so that

$$[\mathcal{H}, m_{op}] = 0 \ , \tag{8}$$

the stationary states can be classified according to the eigenvalues of m_{op},

$$m = 0, 1, 2, \ldots \tag{9}$$

denoting the number of spin deviations. S_0^z [Eq. (7)] corresponds to the ground state, so that

$$S_0^z = -sN, \quad s = \tfrac{1}{2}, 1, \ldots \ . \tag{10}$$

$m = 0$ corresponds to the ground state, and the $m = 1$ space is diagonalized by simple magnons. For the IH and the AEH models, $m = 2$ corresponds to a two-magnon-exchange bound state, as shown by Bethe,[14] Wortis,[20] and Hanus[21] for the IH, and by Orbach[22] and Gochev[23] for the AEH. In the IH, also the $m = 3$,[24] and in the AEH, even the mth bound-state energies have been derived.[23] The $m = 2, 3, 4, 5$ bound states have been observed by Torrance and Tinkham[25] in the strongly anisotropic chain $CoCl \cdot 2H_2O$, which seems to be well described by the $s = \frac{1}{2}$ AEH model. The $m = 2$ bound states of the EAH have been studied by Silberglitt and Torrance.[26] There is an exchange and a single-ion bound state. Recently, the AEH with $s = \frac{1}{2}$ was also treated with the quantum inverse-scattering method.[19]

The classical and continuum limit of the Hamiltonian [Eqs. (1), (2), and (4)] is obtained by replacing the spin operators $\vec{S}_l$ by vectors with slowly varying orientations from site to site, so that

$$\vec{S}_{l+1} - \vec{S}_l = \frac{\partial \vec{S}(x)}{\partial x} a \tag{11}$$

and

$$H = \int H \, dx \ , \tag{12}$$

where the Hamiltonian densities are given by IH:

$$H = \frac{J}{2}\left(\frac{\partial \vec{S}}{\partial x}\right)^2 + hS^z \ , \tag{13}$$

EAH:

$$H = \frac{J}{2}\left(\frac{\partial \vec{S}}{\partial x}\right)^2 - D(S^z)^2 + hS^z \ , \tag{14}$$

AEH:

$$H = \frac{J}{2}\left(\frac{\partial \vec{S}}{\partial x}\right)^2 + \frac{1-g}{g}\left[\left(\frac{\partial S^x}{\partial x}\right)^2 + \left(\frac{\partial S^y}{\partial x}\right)^2\right] - J\left(\frac{g-1}{g}\right)(S^z)^2 \ . \tag{15}$$

The classical vector field $\vec{S}(x)$ satisfies

$$\vec{S}(x)^2 = S^2 \ , \tag{16}$$

and the length will be measured in units of the lattice spacing. The equation of motion for the classical spin field is[7,10]

$$-\hbar \frac{d\vec{S}}{dt} = \vec{S} \times \frac{\delta \mathcal{H}}{\delta \vec{S}} \ , \tag{17}$$

which is, according to Eqs. (13)–(15) dispersive and nonlinear.

A remarkable feature of the classical equation of motion associated with the continuum version of the IH-, AEH-, and EAH-continuum systems is the exact integrability, as demonstrated by the inverse-scattering transform.[12,13] In fact, the systems considered here represent special cases of the exactly integrable Landau-Lifshitz model.[13] Accordingly, there exist one-soliton and multisoliton solutions, the Hamiltonians can be expressed in terms of action angle variables and an infinite series of constants of motion can be constructed.[13,27,28]

This short and certainly incomplete review is enough to indicate that the IH, the EAH, and the AEH chains represent suitable models to investigate the connection between the quantum-mechanical excitation spectrum and the soliton solutions of the associated classical continuum models. The purpose of the paper is to clarify this connection. In Sec. II A, we use the Dyson-Maleev[29,30] boson representation of the Hamiltonians, classify the states, and review the one- and two-spin deviation problems from the point of view of the eigenvalue spectrum. In Sec. II B, we introduce a two-spin Green's function to study the two-magnon bound states and some of their implications at $T = 0$. In Sec. II C, we treat the continuum and weak-coupling limits and establish the mapping of the AEH and EAH models on the Bose gas with attractive δ-function interaction. On this basis, the eigenvalues of the mth bound state can be calculated. Section II D is devoted to the classical and low-temperature limits. It is shown that the bound-state resonance in the imaginary part of the two-spin Green's function survives the classical limit. Its separation from the bottom of the two-magnon continuum is shown to be proportional to T^2. Moreover, as in the quantum case, the presence of the bound-state resonance removes the singularities occurring in the noninteracting case at the bottom and top of the two-magnon continuum. The T^2 dependence of the bound-state resonance implies that, in calculations of the magnon self-energy, performed to order T only,[9] the bound-state effects, resulting from the nonlinearities (solitons) are not yet included.

In Sec. III A, we consider the classical continuum counterparts of the IH, AEH, and EAH models, and summarize those properties of the one-soliton solutions, necessary to quantize them according to the Bohr-Sommerfeld–de Broglie rules. This quantization of the classical one-soliton solutions is performed in Sec. III B. In the IH model, for $s=\frac{1}{2}$ we find exact agreement with the full quantum results. We also substantiate the conjecture that the agreement remains for general s, provided the wave number is sufficiently small. In the AEH and EAH models, the agreement with the quantum results, as obtained from the mapping to the Bose gas in the continuum and weak-coupling limit, is complete for large quantum numbers m, and in the EAH case, for $s >> \frac{1}{2}$, in addition.

We conclude, therefore, that the envelope soliton solutions considered here give rise to bound-state resonances and associated effects in a classical treatment. These effects include the removal of square-root singularities in the continuum of the two-spin Green's function and well-behaved magnon self-energies. In fact, the existence of well-defined magnon resonances at finite temperature can be explained only by taking the "bound states" into account. Moreover, the semiclassical quantization of the envelope soliton solutions leads to remarkable agreement with the exact energy eigenstates. Because the existence of the bound states in the IH, AEH, and EAH models is not restricted to one space dimension,[20,21,26] we conjecture that the bound-state soliton correspondence might also persist in the two- and three-dimensional counterparts. In these dimensions, however, soliton solutions have not yet been found.

II. MAGNONS AND BOUND STATES

In Sec. II A, we introduce the Dyson-Maleev representation[29,30] and summarize the classification of the states of the model system in terms of magnons and bound states. Two-spin Green's functions are introduced in Sec. II B to study the two-magnon bound states and their implications at $T=0$. Continuum and weak-coupling limits and the mappings on the Bose gas with attractive δ-function interaction are considered in Sec. II C. In these limits, the eigenvalue spectrum for the AEH and EAH systems is determined for the mth bound state and any s value. In Sec. II D, we discuss the classical limit of the two-spin Green's function in the continuum and weak-coupling limits for the AEH and EAH models to leading order in T. The bound-state resonance is found to survive the classical limit, but the binding energy is proportional to T^2, in leading order.

A. Dyson-Maleev representation and classification of the states

The Dyson-Maleev transformation gives a correspondence between any operator O on the Hilbert space of the spin system, and an operator $\tilde{O}$ on a boson Hilbert space.[29,30] In particular, for the spin operators we have the following corresponding boson operators:

$$S_i^z=-s+a_i^\dagger a_i \ , \tag{18}$$

$$S_i^\dagger=S_i^x+iS_i^y=(2s)^{1/2}a_i^\dagger\left(1-\frac{a_i^\dagger a_i}{2s}\right) \ , \tag{19}$$

$$S_i^-=S_i^x-iS_i^y=(2s)^{1/2}a_i \ , \tag{20}$$

where

$$[a_i,a_j^\dagger]=\delta_{ij}, \quad [a_i,a_j]=[a_i^\dagger,a_j^\dagger]=0 \ . \tag{21}$$

A limitation of this transformation consists in unphysical states, where a given spin may effectively be flipped more than $2s+1$ times. This issue will be discussed in Sec. II B.

Using the Fourier transformation

$$a_l=\frac{1}{\sqrt{N}}\sum_k e^{-ikl}a_k \ , \tag{22}$$

we write the Hamiltonians (1), (2), and (4) in terms of bosons, and obtain

$$\mathcal{H}=E_0+\sum_k \omega_k a_k^\dagger a_k + \frac{1}{N}\sum_{k_1,k_2,q} v(k_1,k_2,q)\,a_{q/2+k_1}^\dagger a_{q/2-k_1}^\dagger \times a_{q/2+k_2}a_{q/2-k_2} \ , \tag{23}$$

where the corresponding ground-state energies and magnon frequencies ω_k are listed in Table I. The magnon interactions $v(k_1,k_2,q)$ are listed in Table II. Since the Hamiltonian commutes with $m_{\rm op}=\sum_l (S_l^z-S_0^z)$ [Eq. (7)], the states of the system can be classified according to the eigenvalues m of $m_{\rm op}$, representing the number of spin deviations. $m=0$ corresponds to the ground state E_0, and the $m=1$ space is diagonalized by the magnons with frequency ω_q, as listed in Table I.

For the IH and AEH chains, the $m>1$ states correspond to m-magnon-exchange bound states, resulting from the magnon interaction $v(k_1,k_2,q)$. The associated bound-state energies were obtained by solving the associated Schrödinger equation by the t-matrix or Green's-function techniques.[14,20–25] Some results for the exchange bound-state frequencies for

TABLE I. Magnon frequencies ω_q and ground-state energies E_0.

	ω_q	E_0
IH	$h+2JS(1-\cos q)$	$-JN_s^2-hNs$
EAH	$h+2D(s-\frac{1}{2})+2Js(1-\cos q)$	$-JNs^2-DNs^2-hNs$
AEH	$h+2Js\left(1-\frac{1}{g}\cos q\right)$	$-\frac{J}{g}Ns^2-hNs$

$s=\frac{1}{2}$ are summarized in Tables III and IV. The two-magnon bound-state frequency may be compared with the bottom of the two-magnon continuum, which occurs for the AEH and $s=\frac{1}{2}$ at

$$\omega_{BC}(q)=2h+2J\left(1-\frac{1}{g}\cos\tfrac{1}{2}q\right) . \quad (24)$$

The two-magnon bound state lies lower than this by a binding "energy"

$$\omega_B(q)=\omega_{BC}(q)-\omega_{m=2}(q)$$

$$=2J\left(1-\frac{1}{g}\cos\tfrac{1}{2}q\right)-J\left(1-\frac{1}{g^2}\cos^2\tfrac{1}{2}q\right) . \quad (25)$$

In the IH, where $g=1$, the binding energy ranges from

$$\tfrac{1}{4}J(\tfrac{1}{2}q)^4 \text{ for } q \ll 1 \quad (26)$$

to

$$J \text{ for } q=\pi . \quad (27)$$

In the AEH model, however, there is a gap in the magnon spectrum, so that the binding energy ranges from

$$J\left(1-\frac{1}{g}\right)^2 \text{ for } q=0 \quad (28)$$

to

$$J \text{ for } q=\pi . \quad (29)$$

The small-q behavior of the binding energy reveals that the two-magnon-exchange bound states appear for arbitrarily small wave numbers. Hence, there is no range of momentum space where the associated nonlinearities can be neglected.

In the EAH chain, the bound-state problem is more complicated, due to the presence of the single-ion anisotropy. This case and the extension to general s values will be considered in Sec. II B.

TABLE II. Magnon interactions [Eq. (23)].

	$v(k_1,k_2,q)$
IH	$-J\cos k_2(\cos k_1-\cos\frac{1}{2}q)$
EAH	$-J\cos k_2(\cos k_1-\cos\frac{1}{2}q)-D$
AEH	$-J\cos k_2\left(\cos k_1-\frac{1}{g}\cos\frac{1}{2}q\right)$

TABLE III. Frequencies of the two- and three-magnon-exchange bound states in the IH for $s=\frac{1}{2}$ (Refs. 14, 20, and 21). For comparison, we included the magnon frequency ($m=1$).

m	ω
1	$h+J(1-\cos q)$
2	$2h+\frac{1}{2}J(1-\cos q)$
3	$3h+\frac{1}{3}J(1-\cos q)$

TABLE IV. Frequencies of the two- and three-magnon-exchange bound states in the AEH for $s=\frac{1}{2}$ (Refs. 22, 23, and 25). For comparison, we included the magnon frequency ($m=1$).

m	w
1	$h+J\left(1-\frac{1}{g}\cos q\right)$
2	$2h+J\left(1-\frac{1}{g^2}\cos^2\frac{1}{2}q\right)$
3	$3h+J\left(1-\frac{1}{g}\frac{2g+\cos q}{4g^2-1}\right)$

B. Two-spin Green's function approach

For our purpose, it is most convenient to study the bound-state problem in terms of the singularities of the two-spin Green's function. In fact, on this basis the significance of $m=2$ bound states in a classical description can be clarified.

We consider the Green's function

$$G_{pp'}(q,\omega)=\langle\langle a_{q/2+p}a_{q/2-p};a^{\dagger}_{q/2+p'}a^{\dagger}_{q/2-p'}\rangle\rangle \quad (30)$$

which, according to Eq. (20), is related to the two-spin Green's function by

$$\langle\langle S^-_p S^-_{q-p};S^{\dagger}_{p'}S^{\dagger}_{q-p'}\rangle\rangle=4s^2G_{pp'}(q,\omega)\ . \quad (31)$$

where we neglected the $a^{\dagger}a^{\dagger}a$ term in Eq. (19). The equation of motion reads[31]

$$-\omega G_{pp'}(q,\omega)=\frac{1}{2\pi}\langle[a_{q/2+p}a_{q/2-p},a^{\dagger}_{q/2+p'}a^{\dagger}_{q/2-p'}]\rangle + \langle\langle[a_{q/2+p}a_{q/2-p},\mathcal{H}];a^{\dagger}_{q/2+p'}a^{\dagger}_{q/2-p'}\rangle\rangle\ . \quad (32)$$

The exact result for the Green's function on the right-hand side is

$$\begin{aligned}\langle\langle[a_{q/2+p}a_{q/2-p},\mathcal{H}];a^{\dagger}_{q/2+p'}a^{\dagger}_{q/2-p'}\rangle\rangle
&=(\omega_{q/2+p}+\omega_{q/2-p})G_{pp'}(q,\omega)+\frac{2}{N}\sum_{k_2}v(p,k_2,q)G_{k_2p'}(q,\omega)\\
&\quad+\frac{2}{N}\sum_{k_1,k_2q'}v(k_1,k_2,q')(\delta_{q/2-p,q'/2+k_1}\langle\langle a_{q'/2-k_1}a_{q/2+p}a_{q'/2+k_2}a_{q'/2-k_2};a^{\dagger}_{q/2+p'}a^{\dagger}_{q/2-p'}\rangle\rangle\\
&\quad+\delta_{q/2+p,q'/2+k_1}\langle\langle a^{\dagger}_{q'/2-k_1}a_{q/2-p}a_{q'/2+k_2}a_{q'/-k_2};a^{\dagger}_{q/2+p'}a^{\dagger}_{q/2-p'}\rangle\rangle)\end{aligned} \quad (33)$$

and the commutator term yields

$$\langle[a_{q/2+p}a_{q/2-p},a^{\dagger}_{q/2+p'}a^{\dagger}_{q/2-p'}]\rangle=(\delta_{p,p'}+\delta_{p,-p'})(1+\langle a^{\dagger}_{q/2+p}a_{q/2+p}\rangle+\langle a^{\dagger}_{q/2-p}a_{q/2-p}\rangle)\ . \quad (34)$$

At low temperature, we may decouple the six-particle Green's function in Eq. (33), according to

$$\langle\langle a^{\dagger}_{q'/2-k_1}a_{q/2\pm p}a_{q'/2+k_2}a_{q'/2-k_2};a^{\dagger}_{q/2+p'}a^{\dagger}_{q/2-p'}\rangle\rangle\approx\delta_{qq'}\delta_{-k_1,\pm p}n_{q/2\pm p}G_{k_2,p'}(q,\omega)\ , \quad (35)$$

where

$$n_p=\langle a^{\dagger}_p a_p\rangle_0=(\exp\beta\omega_p-1)^{-1}\ . \quad (36)$$

Here, we neglected the other two decoupling terms corresponding to the pairing of $a^{\dagger}$ with the other two operators. It is easily verified that these terms are proportional to $G_{pp'}$ and merely renormalize the bare magnon frequencies in the first term of Eq. (33). The equation of motion (32) then reduces to the integral equation

$$G_{pp'}(q,\omega)=G^0_{pp}(q,\omega)\delta_{p,p'}+G^0_{pp}(q,\omega)\frac{2\pi}{N}\sum_{k_2}v(p,k_2,q)G_{k_2p'}(q,\omega)\ , \quad (37)$$

where

$$G^0_{pp}=-\frac{1}{\pi}\frac{1+n_{q/2+p}+n_{q/2-p}}{\omega+\omega_{q/2+p}+\omega_{q/2-p}}\ . \quad (38)$$

The decoupling [Eq. (35)] and the resulting integral equation (37) are exact at $T=0$, due to the antinormal ordering of the operators, and the fact that the ground state is the boson vacuum. For finite but low temperatures, the approximation is valid to leading order in a magnon-density expansion.

In this section, we consider the zero-temperature case only, where $n_p=0$ [Eq. (36)]. Introducing the kernel

$$v(k_1,k_2,q)=-J\cos k_2\left(\cos k_1-\frac{1}{g}\cos\tfrac{1}{2}q\right)-D\ , \qquad (39)$$

which includes the IH, EAH, and AEH kernels as special cases (Table II), the solution of the integral equation (37) is readily obtained,

$$G(q,\omega)=\frac{G^0(q,\omega)[1+2\pi JR(q,\omega)]-2\pi JC(q,\omega)B(q,\omega)}{1+L(q,\omega)}\ , \qquad (40)$$

$$G(q,\omega)=\left\langle\left\langle\frac{1}{\sqrt{N}}\sum_p a_{q/2+p}a_{q/2-p};\frac{1}{\sqrt{N}}\sum_p a^\dagger_{q/2+p}a^\dagger_{q/2-p}\right\rangle\right\rangle\ , \qquad (41)$$

$$G^0(q,\omega)=\frac{1}{N}\sum_p G^0_{pp}(q,\omega),\quad G^0_{pp}(q,\omega)=-\frac{1}{\pi}\frac{1}{\omega+\omega_{q/2+p}+\omega_{q/2-p}}\ , \qquad (42)$$

$$B(q,\omega)=\frac{1}{N}\sum_p G^0_{pp}(q,\omega)\cos p,\quad C(q,\omega)=\frac{1}{N}\sum_p G^0_{pp}(q,\omega)\left(\cos p-\frac{1}{g}\cos\tfrac{1}{2}q\right)\ ,$$

$$R(q,\omega)=\frac{1}{N}\sum_p G^0_{pp}(q,\omega)\cos p\left(\cos p-\frac{1}{g}\cos\tfrac{1}{2}q\right)\ , \qquad (43)$$

$$1+L(q,\omega)=[1+2\pi DG^0(q,\omega)][1+2\pi JR(q,\omega)]-4\pi^2JDC(q,\omega)B(q,\omega)\ , \qquad (44)$$

$$\omega_p=h+2D(s-\tfrac{1}{2}+2Js\left(1-\frac{1}{g}\cos q\right)\ . \qquad (45)$$

To estimate the limitations of Dyson-Maleev representation [Eqs. (18)–(20)], namely, the appearance of unphysical states where a spin may effectively be flipped more than $2s+1$ times, we calculated the Green's function defined by Eq. (31) also direct at $T=0$, again using the equation-of-motion technique. Following Wortis,[20] we obtain

$$\left\langle\left\langle\frac{1}{\sqrt{N}}\sum_p S^-_{q/2+p}S^-_{q/2-p};\frac{1}{\sqrt{N}}\sum_{p'} S^+_{q/2+p'}S^+_{q/2-p'}\right\rangle\right\rangle=\left\langle\left\langle\frac{1}{\sqrt{N}}\sum_q (s_l^-)^2e^{iql};\frac{1}{\sqrt{N}}\sum_q (s_l^+)^2e^{-iql}\right\rangle\right\rangle$$

$$=4s^2\left(1-\frac{1}{2s}\right)G(q,\omega)\ , \qquad (46)$$

where $G(q,\omega)$ is given by Eq. (40). From Eqs. (19), (20), (30), and (31), it is seen that the $(1-1/2s)$ prefactor is missing by using the Dyson-Maleev representation and by neglecting the $a^\dagger a^\dagger a$ terms in Eq. (19). We note, however, that the inclusion of this term leads to Eq. (46) so that the Dyson-Maleev representation becomes exact at $T=0$ and even for $s=\frac{7}{2}$.

To unravel the resonance structure of the imaginary part of $G(q,\omega)$ we substitute

$$\omega\to\omega-i\epsilon \qquad (47)$$

and perform the sums in terms of integrals. Setting $D=0$, we obtain

$$G''=\frac{G^{0''}(1+2\pi JR')^2+4\pi^2J^2R''C'B'-2\pi J(1+2\pi JR')(C'B''+B'C'')}{(1+2\pi JR')^2+4\pi^2J^2R''^2} \qquad (48)$$

for

$$-\omega \geq 2h + 4JS\left[1 - \frac{1}{g}\cos\tfrac{1}{2}q\right] = \omega_{BC}(q) \ , \quad (49)$$

where

$$B''(q,\omega) = G^{0\prime\prime}(q,\omega)a(q,\omega) \ ,$$

$$C''(q,\omega) = G^{0\prime\prime}(q,\omega)\left[a(q,\omega) - \frac{1}{g}\cos\tfrac{1}{2}q\right] \ ,$$

$$R''(q,\omega) = G^{0\prime\prime}(q,\omega)\,a(q,\omega)\left[a(q,\omega) - \frac{1}{g}\cos\tfrac{1}{2}q\right] \ , \quad (50)$$

$$G^{0\prime\prime}(q,\omega) = -\frac{1}{\pi}\left[\frac{4JS}{g}\cos\tfrac{1}{2}q\right]^{-1}[1 - a^2(q,\omega)]^{-1/2} \ , \quad (51)$$

$$a(q,\omega) = g\frac{\omega + 2h + 4JS}{4JS\cos\frac{1}{2}q} \ , \quad (52)$$

$$B'(q,\omega) = C'(q,\omega) = \frac{1}{\pi}\left[\frac{4JS}{g}\cos\tfrac{1}{2}q\right]^{-1} \ ,$$

$$R'(q,\omega) = B'(q,\omega)\left[a(q,\omega) - \frac{1}{g}\cos\tfrac{1}{2}q\right] \ , \quad (53)$$

$$G^{0\prime}(q,\omega) = 0 \ .$$

Below the bottom of the continuum,

$$-\omega \leq \omega_{BC}(q) \ ,$$

we find

$$G''(q,-\omega) = -2\pi^2 JC'(q,-\omega)B'(q,-\omega) \times \delta(1 + 2\pi JR'(q,-\omega)) \ , \quad (54)$$

where

$$B'(q,-\omega)C'(q,\omega) = \left[\frac{g}{\pi 4Js\cos\frac{1}{2}q}\right]^2\left[1 - \frac{a(q,\omega)}{[a^2(q,\omega)-1]^{1/2}}\right] \times\left[1 + \frac{1}{g}\frac{\cos\frac{1}{2}q}{[a^2(q,\omega)-1]^{1/2}} - \frac{a(q,\omega)}{[a^2(q,\omega)-1]^{1/2}}\right] \ , \quad (55)$$

$$2\pi JR'(q,-\omega) = -\frac{1}{2s}\left[1 - \frac{a(q,\omega)}{[a^2(q,\omega)-1]^{1/2}}\right] \times\left[1 - \frac{ga(q,\omega)}{\cos\frac{1}{2}q}\right] \ .$$

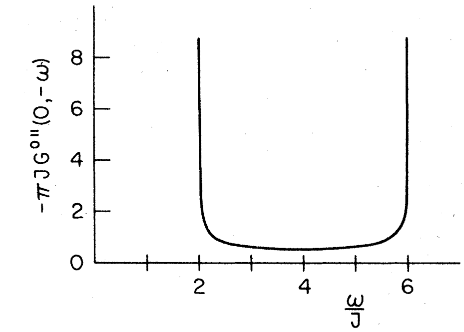

FIG. 1. Frequency dependence of the imaginary part of the two-spin Green's function [Eq. (51)] for the AEH chain for $s=1$, $g=2$, $h=0$, and $q=0$. The square-root singularities occur at $\omega/J=2$ and 6. These values correspond to the bottom and top of the two-magnon continuum.

From Eq. (54), we see that the energy of the two-magnon-exchange bound state follows from the condition

$$1 + 2\pi JR'(q,\omega) = 0 \ . \quad (56)$$

In the noninteracting case $G''(q,\omega)$ [Eq. (51)] exhibits square-root singularities at energies corresponding to the bottom and top of the continuum. These features are illustrated in Fig. 1 for the AEH chain. The profound modifications resulting from the interaction are seen in Fig. 2 for the same system. Not only is there the bound-state resonance [Eq. (56)], but also the continuum resonance is dramatically modified, due to the removal of the square-root singularities [Eq. (51)].

The bound-state energy resulting from Eq. (56) is the easiest to calculate analytically when $s=\frac{1}{2}$, in

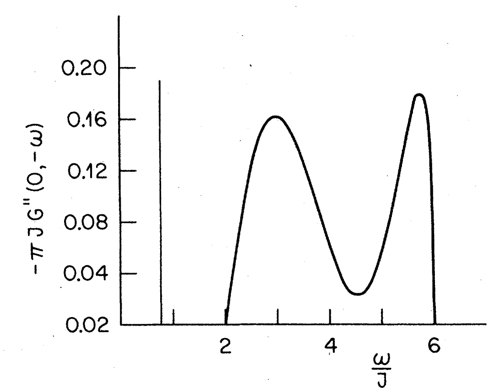

FIG. 2. Frequency dependence of the imaginary part of the two-spin Green's function [Eqs. (48) and (54)], for the AEH chain for $s=1$, $g=2$, $h=0$, and $q=0$. The δ function represents the bound-state resonance occurring at $\omega/J=0.75$ [Eq. (57)].

which case we find

$$-\omega = 2h + J\left(1 - \frac{1}{g^2}\cos^2\tfrac{1}{2}q\right) , \qquad (57)$$

consistent with the corresponding expression given in Table III.

In the IH chain ($g=1$), the effect of the bound-state resonance on $G''(q,\omega)$ is quite similar to $g \neq 0$. For $q=0$, however, there is no bound state in this case [Eqs. (24)–(27)].

Finally, we turn to the EAH chain, where $D \neq 0$ and $g=1$. Here, in analogy to Eq. (56), the bound-state frequencies follow from

$$1 + L'(q, -\omega) = 0 . \qquad (58)$$

As pointed out by Silberglitt and Torrance,[26] there are two bound-state solutions for $q \neq 0$. This is easiest to show for $q=\pi$, where $C(q,\omega)$ and $B(q,\omega)$ in Eq. (44) vanish. From Eqs. (45), (46), and (58), we find

$$-\omega_{q=\pi} = 2h + 4Js + 4D(s - \tfrac{1}{2}) - J \qquad (59)$$

and

$$-\omega_{q=\pi} = 2h + 4Js + 4D(s - \tfrac{1}{2}) - 2D . \qquad (60)$$

The first expression is the energy of the two-magnon-exchange bound state, while Eq. (60) corresponds to the two-magnon single-ion bound-state energy. For $q=\pi$, the top and the bottom of the two-magnon continuum merge to the single energy,

$$-\omega_{q=\pi} = 2h + 4Js + 4D(s - \tfrac{1}{2}) . \qquad (61)$$

At $q=0$, however, only the single-ion bound state survives. In the weak-coupling limit defined by

$$\frac{D}{2Js} \ll 1 , \qquad (62)$$

we find from Eqs. (44), (45), and (58), the solution

$$-\omega_{q=0} = 2h + 4D(s - \tfrac{1}{2}) - \frac{D^2}{2Js}\left(1 - \frac{1}{2s}\right)^2 \qquad (63)$$

corresponding to the energy of the single-ion bound state. A numerical solution of Eq. (58) reveals that for $h=0$, $D=1$, and $s=1$, the exchange bound state does not appear until $q \gtrsim \frac{5}{2}\pi$.[26] The essential effects of the bound states on $G''(q,-\omega)$ are according to Eq. (40), similar to those outlined in the AEH chain (Figs. 1 and 2). The appearance of the bound-state resonances removes the square-root singularities occurring in the continuum of the noninteracting case.

C. Continuum and weak-coupling limits; mappings to the Bose gas

In this section, we treat the continuum limit of the AEH and IH models to establish a mapping on the Bose gas with attractive δ-function interactions. The continuum limit is obtained by replacing the magnon frequencies listed in Table I by the Taylor expanded expressions up to second order. Moreover, we replace the interaction terms $v(k_1,k_2,q)$ (Table II) by their long-wavelength limits.

Hamiltonian (23) then simplifies to

$$\mathcal{H} = E_0 + \sum_k \omega_k a_k^\dagger a_k + r\frac{1}{N}\sum_{k_1,k_2,q} a_{q/2+k_1}^\dagger a_{q/2-k_1}^\dagger a_{q/2+k_2} a_{q/2-k_2} , \qquad (64)$$

where

$$r = \begin{cases} -D: \text{ EAH} & (65) \\ -J(1-1/g): \text{ AEH} . & (66) \end{cases}$$

In this limit, the solution of the integral equation (37) becomes trivial, because the originally nonlocal interaction $v(p,k_2,q)$ becomes a constant. The solution is

$$G(q,\omega) = \frac{G^0(q,\omega)}{1 - 2\pi r G^0(q,\omega)} , \qquad (67)$$

where

$$G^0(q,\omega) = -\frac{1}{2\pi^2}\int_{-\Delta}^{+\Delta} \frac{dp}{\omega + \omega_{q/2+p} + \omega_{q/2-p}} , \qquad (68)$$

and according to Table I,

$$\omega_q = \begin{cases} h + 2D(s - \tfrac{1}{2}) + Jsq^2: \text{ EAH} & (69) \\ h + 2Js(1-1/g) + (Js/g)q^2: \text{ AEH} . & (70) \end{cases}$$

Δ denotes a cutoff. The bound-state condition (58) then reduces for $q=0$ to

$$I - 2\pi r G^{0\prime}(0, -\omega) = 0 , \qquad (71)$$

by replacing ω in Eq. (68) by $\omega - i\epsilon$. Using Eqs. (68)–(71), we find for the bound-state frequencies,

$$-\omega_{q=0} = \begin{cases} 2h + 4D(s - \tfrac{1}{2}) - D^2/2Js: \text{ EAH} & (72) \\ 2h + 4Js(1-1/g) - J(1-1/g)^2 g/2s: \text{ AEH} . & (73) \end{cases}$$

These results can now be compared with the corresponding exact expressions given in Eqs. (57) and (63), where relation (63) is valid only in the weak-coupling limit ($D/2Js \ll 1$).

Considering first the EAH case, we see from Eqs. (63) and (72) that the continuum limit is valid in the weak-coupling limit for $2s \gg 1$. The latter condition can be removed by introducing the "renormalized" single-ion anisotropy constant

$$D \to D\left(1 - \frac{1}{2s}\right) \qquad (74)$$

in the D^2 term of Eq. (72). In the AEH case, we introduce

$$g = 2\epsilon^2 + 1 \ , \tag{75}$$

and assume small exchange anistropy

$$\epsilon \ll 1 \ . \tag{76}$$

In this case, Eq. (73) reduces to

$$-\omega = 2h + 8sJ\epsilon^2 \left[1 - 2\epsilon^2 - \frac{1}{4s^2}\epsilon^2 \right] \ . \tag{77}$$

This expression agrees for $s = \frac{1}{2}$ and to fourth order in ϵ with the expanded exact result [Eq. (57)].

In both cases, therefore, the continuum limit reproduces the exact bound-state expressions at $q = 0$ in the appropriate weak-coupling limits [Eqs. (62) and (76)], where in the EAH case, D has to be renormalized [Eq. (74)]. This behavior may be understood by recognizing that the continuum approximation assumes spatially slowly-varying spin fluctuations, guaranteed only for weak coupling, or in other words, close to the Heisenberg limit. The effect of the bound state on the imaginary part of the Green's function also becomes particularly transparent in this limit. Using Eqs. (47) and (67), we find

$$G''(q, -\omega) = \frac{G^{0''}(q, -\omega)}{[1 - 2\pi r G^{0'}(q, -\omega)]^2 + [2\pi r G^{0''}(q, -\omega)]^2} \ . \tag{78}$$

For $q = 0$, it follows from Eq. (68) that

$$\begin{aligned} G^{0''}(0, -\omega) &= 0, \quad -\omega < 2\omega_{q=0} \ , \\ G^{0'}(0, -\omega) &= 0, \quad -\omega > 2\omega_{q=0} \ , \end{aligned} \tag{79}$$

so that for $-\omega < 2\omega_{q=0}$,

$$G''(0, -\omega) = \frac{1}{2\pi r}\delta(1 + 2\pi r G^{0'}(0, -\omega)) \ , \tag{80}$$

and for $\omega > 2\omega_{q=0}$,

$$G''(0, -\omega) = \frac{G_0''(0, -\omega)}{1 + \left[2\pi r G^{0''}(0, -\omega)\right]^2} \ . \tag{81}$$

Equation (80) describes the bound-state resonances, and Eq. (81) the modified resonance structure of the two-magnon continuum at and above $\omega = 2\omega_{q=0}$. The denominator in Eq. (81) removes the square-root singularities appearing for $r = 0$. This behavior has already been illustrated in Fig. 2, but the present analysis extends the picture to the EAH model at $q = 0$.

Finally, we turn to the mapping of the AEH and EAH models on the nonrelativistic m-body Schrödinger equation with attractive δ-function interaction. The Hamiltonian of this system reads

$$\mathcal{H} = ma + \sum_{i=1}^{m} -\frac{1}{2}\frac{\partial^2}{\partial x_i^2} - b \sum_{j>i=1}^{m} \delta(x_j - x_i) \ , \tag{82}$$

where m denotes the number of Bose particles. The associated Schrödinger equation has been solved exactly by McGuire.[32] He finds that, in addition to the elementary boson, the system possesses a single bound state of m bosons for each value of m, with energy

$$\omega(m) = ma - \tfrac{1}{12}b^2 m(m^2 - 1) \ . \tag{83}$$

In the second quantized form, the Hamiltonian (82) reads

$$\mathcal{H} = ma + \sum_k k^2 a_k^\dagger a_k - \tfrac{1}{2}b \sum_{k_1 k_2 q} a_{q/2+k_1}^\dagger a_{q/2-k_1}^\dagger a_{q/2+k_2} a_{q/2-k_2} \tag{84}$$

which is equivalent to Eq. (64), with ω_k replaced by the continuum expressions (69) and (70). This equivalence establishes the mapping of the EAH and AEH models to the Bose gas with attractive δ-function interaction. Clearly, the mapping only holds in the continuum and weak-coupling limits. Using

TABLE V. Frequencies of the magnon ($m = 1$) and m-magnon bound states for $q = 0$, in the weak-coupling [Eqs. (62), (75), and (76)] and continuum limits, according to the mapping on the Bose gas with attractive δ-function interaction.

	ω_m ($q = 0$)
EAH	$mh + 2mD(s - \frac{1}{2}) - \frac{1}{12}m(m^2 - 1)\frac{D^2}{Js}\left[1 - \frac{1}{2s}\right]$
AEH	$mh + 4Jsm\epsilon^2\left[1 - 2\epsilon^2 - \frac{(m^2 - 1)\epsilon^2}{12s^2}\right]$

Eqs. (64)–(66), (69), (70), (83), and (84), the frequencies of the mth bound state in the EAH and AEH systems are now readily calculated. The results are given in Table V and are used later on for comparison with the Bohr-Sommerfeld quantized soliton energies. Moreover, these results extend the formerly known $s=\frac{1}{2}$ bound states in the AEH model[23] to general s, and in the EAH model, the known single-ion bound state[26] to arbitrary bound-state configurations.

D. Classical limit

We note that solution (40) of the integral equation (37) also holds at finite T to leading order in the magnon density, provided G^0_{pp} in Eqs. (40)–(45) is replaced by Eq. (38). The classical limit is then easily obtained by setting

$$n_p=(\exp\beta\omega_p-1)^{-1}\to\frac{T}{\omega_p}\ ,\qquad n_p+1\to\frac{T}{\omega_p}\ . \tag{85}$$

Substitution into Eq. (38) yields the classical result

$$G^0_{pp}(q,\omega)=-\frac{T}{\pi}\left[\frac{1}{\omega_{q/2+p}}+\frac{1}{\omega_{q/2-p}}\right]\frac{1}{\omega+\omega_{q/2+p}+\omega_{q/2-p}}\ , \tag{86}$$

valid to leading order in T. It is important to emphasize that from a quantum-mechanical point of view, Eqs. (85) and (86) represent a high-temperature approximation ($\beta\omega_q\ll 1$). In this sense, the classical limit becomes somewhat academic at low T. Nevertheless, for theoretical purposes, it is still useful to consider the classical limit at low T, to clarify the connection between quantum-mechanical bound states and solitons, to compare with classical low-temperature expansions,[9] and to interpret molecular-dynamics results.[6–8] The classical limit of $G(q,\omega)$ is then obtained by substituting Eq. (86) into Eqs. (40)–(45). Because the condition for a bound-state resonance remains unaltered [Eq. (58)], it is clear that its occurrence in $G(q,-\omega)$ will survive the classical limit. This is the most easily demonstrated in the continuum and weak-coupling limits for the AEH and EAH systems. From Eqs. (67), (69)–(71), and (86), we find to leading order in T,

$$-\omega_{q\to 0}=\begin{cases}2h+8Js\epsilon^2\left[1-2\epsilon^2-\dfrac{\epsilon^2}{4s^2}\left[\dfrac{T}{h}\right]^2\right]:\ \text{AEH} & (87)\\[2ex] 2h+4D(s-\frac{1}{2})-\dfrac{D^2}{2Js}\left[1-\dfrac{1}{2s}\right]^2\left[\dfrac{2T}{2h+4D(s-\frac{1}{2})}\right]^2:\ \text{EAH}\ . & (88)\end{cases}$$

The existence of these solutions confirms the existence of two-magnon bound-state resonances in $G''(q,\omega)$ in the classical limit. The only, but crucial, difference from the quantum case at $T=0$, is the T^2 dependence of the binding energy for $q\neq\pi$. As a consequence, any classical calculation of the magnon self-energy needs to be correct at least to order T^2, to include the bound-state effects. Thus, these effects were not included in the work of Reiter and Sjölander[9] for the IH chain, where the magnon self-energy was calculated to order T.

As illustrated in Fig. 3, the presence of the bound-state resonances affects $G''(q,\omega)$ as in the quantum treatment (Fig. 2) by removing the square-root singularities appearing in the two-magnon continuum by neglecting the magnon interaction. Moreover, the high-frequency part of the continuum is considerably reduced in comparison to the $T=0$ quantum case (Fig. 2) due to the thermal weight $2T/\omega_p$.

At this point, it is important to emphasize again that the bound-state resonance and the associated effects are a consequence of the magnon interaction or, in other words, of the inherent nonlinearity, which

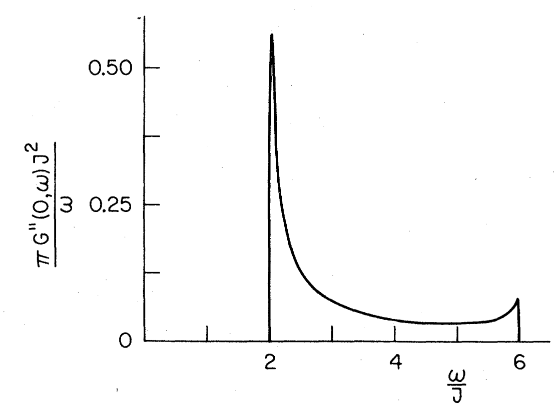

FIG. 3. Frequency dependence of the imaginary part of the two-spin Green's function [Eqs. (48) and (86)] for the AEH chain for $T/J=0.1$, $h/J=0$, $s=1$, $g=2$, and $q=0$ in the classical limit. The "bound-state energy" is given by $\omega/J=2-\frac{1}{4}(T/J)^2$.

also gives rise to the soliton solutions in the continuum limit. From the structure of $G''(0,\omega)$, it now becomes clear that in the classical limit the origin of the bound-state resonances and their effects on the continuum may also be identified as soliton features.

III. SOLITONS AND BOHR-SOMMERFELD–DE BROGLIE QUANTIZATION

In Sec. III A, we consider the classical and continuum counterparts of the IH, AEH, and EAH chains, and summarize those properties of the one-soliton solutions necessary to perform the Bohr-Sommerfeld–de Broglie quantization, outlined in Sec. III B.

A. One-soliton solutions

The classical counterparts of the Heisenberg chains treated in Sec. II, are defined by the Hamiltonian densities given in Eqs. (13)–(15), the equation of motion (17) and conditions (16) for the classical spin field. A remarkable feature of all three models is the exact integrability,[12,13] associated with soliton solutions and an infinite number of conservation laws.

For our purpose, it is sufficient, however, to consider the one-soliton solutions, and as far as conserved quantities are concerned, we consider the energy, the magnetization, and the field momentum. Introducing the polar coordinates

$$\vec{S}=s[(1-u^2)^{1/2}\cos\phi,(1-u^2)^{1/2}\sin\phi,u] \quad , \tag{89}$$

where

$$u=\cos\theta \quad , \tag{90}$$

the Lagrange density is

$$L=\hbar s(1-u)\dot{\phi}-H \tag{91}$$

TABLE VI. Boundary conditions and value of the momentum Lagrange multiplier.

		$x=\pm\infty$	v
IH		$\theta_x=0,\ \theta=0$	$\neq 0$
AEH	$\phi_x=0$	$\theta_x=0,\ \theta=0$	0
EAH	$\phi_x=0$	$\theta_x=0,\ \theta=0$	0

and the equation of motion (17) reduces to

$$\hbar\dot{u}=+\frac{1}{s}\frac{\delta\mathcal{H}}{\delta\phi},\quad \hbar\dot{\phi}=-\frac{1}{s}\frac{\delta\mathcal{H}}{\delta u} \quad . \tag{92}$$

By symmetry, conserved quantities are the magnetization [Eq. (8)],

$$M^z=s\int(1-u)\,dx=\frac{1}{h}\int\frac{\partial L}{\partial\dot{\phi}}\,dx \quad , \tag{93}$$

the field momentum

$$P=\int\phi_x\frac{\partial L}{\partial\dot{\phi}}\,dx=s\hbar\int dx\,\phi_x(1-u) \tag{94}$$

and the energy. Introducing the Lagrangian multipliers Ω and v, the governing equations of motion can also be obtained by minimizing[10]

$$I(\Omega,v;u,\phi)=\int H\,dx-\hbar\Omega M^z-v(P-P_0) \tag{95}$$

with respect to u and ϕ. In fact, if we compare

$$\begin{aligned}\frac{\delta I}{\delta u}&=\frac{\delta\mathcal{H}}{\delta u}-s\hbar\Omega+v\hbar s\frac{\partial\phi}{\partial x}=0 \quad ,\\ \frac{\delta I}{\delta\phi}&=\frac{\delta\mathcal{H}}{\delta\phi}-v\hbar s\frac{\partial u}{\partial x}=0 \quad ,\end{aligned} \tag{96}$$

with the equations of motion (92), we see that we are

TABLE VII. Energy E and magnetization M^z associated with the one-soliton solution, consistent with the boundary conditions given in Table VI.

IH	$E=\frac{16}{M^z}Js^3\sin^2\frac{P}{4s\hbar}+hM^z$
EAH	$\tan\frac{1}{2}\theta=\left[\frac{2Ds-\hbar\Omega}{\Omega h}\right]^{1/2}\left\{\cosh\left[\left[\frac{2D}{J}\right]^{1/2}\left[\frac{2Ds-\hbar\Omega}{2Ds}\right]^{1/2}(x-x_0)\right]\right\}^{-1}$
	$E=4s^2(2DJ)^{1/2}\left[\frac{2Ds-\hbar\Omega}{2D}\right]^{1/2}$
	$M^z=4s\left[\frac{J}{2D}\right]^{1/2}\operatorname{arccosh}\left[\frac{2Ds}{\hbar\Omega}\right]^{1/2}$
AEH	As in EAH with $D\rightarrow J\left[1-\frac{1}{g}\right]$

essentially finding solutions of the solitary wave form

$$u(x,t)=u(x-vt), \quad \phi=\Omega t+\varphi(x-vt) \quad . \qquad (97)$$

The boundary conditions of interest and the value of the Lagrange multiplier associated with the momentum are given in Table VI. The resulting envelope soliton solution in the IH model is well documented[3,10,12] and we merely quote the associated energy in Table VII. In the EAH and AEH models, we consider solitons with $v=0$ only (Table VI). The solution consistent with the boundary conditions (Table VI), together with the associated energy and magnetization are given in Table VII. Up to the substitution $D \leftrightarrow J(1-1/g)$ the results for the EAH and AEH systems are identical. The soliton corresponds to a bound kink-antikink pair, where the energy of the sine-Gordon-like kink is given by $2S^2(2DJ)^{1/2}$. These kink solutions do not exist, however, for $v \neq 0$.[33]

B. Bohr-Sommerfeld–de Broglie quantization of the solitons

In view of the fact that both the soliton solutions of the classical equations of motion and the bound states of the quantum-mechanical description are a consequence of the nonlinearity, we expect the solitons in the systems considered here to be closely related to the quantum bound states. This conjecture has already been substantiated in Sec. II D, where we found that the bound-state resonance survives the classical limit. Moreover, in the case of the IH model, it was shown that the WKB quantization of the envelope solitons leads to the quantum energy states.[34,35] Fortunately, there is a much simpler approach at hand for this, namely, the Bohr-Sommerfeld–de Broglie quantization rules of the old quantum theory.[36]

In the EAH and AEH models, where the linear momentum P does not enter the soliton energy (Table VII), because we assumed $v=0$ (Table VI), we might use the following Bohr-Sommerfeld quantization rule: If we have a family of periodic motions, labeled by the period $T=2\pi/\Omega$, then an energy eigenstate occurs whenever

$$\int_0^T dt \int dx\, P_\phi \dot{\phi}=2\pi m \quad , \quad m=0,1,2,3,\ldots, \qquad (98)$$

where

$$P_\phi=\frac{\partial L}{\partial \dot{\phi}}=\hbar s(1-u) \qquad (99)$$

is the canonically conjugate momentum to ϕ. For our purpose, it is more convenient to use the related correspondence between classical energy and quantum frequency,[36] valid for large m,

$$\frac{1}{\hbar}\frac{dE}{dm}=\Omega(E) \quad . \qquad (100)$$

Applying this formula to the EAH and AEH soliton energies (Table VII) and using as a boundary condition that $E=0$ for $m=0$, we find

$$E(m)=4s^2\sqrt{2DJ}\,\tanh\frac{m}{2S}\left(\frac{2D}{J}\right)^{1/2} \quad . \qquad (101)$$

The requirement of a positive classical oscillation frequency leads to

$$\frac{m}{2S}\left(\frac{2D}{J}\right)^{1/2}<\infty \quad , \qquad (102)$$

so that the integers m can assume any value. This property is very different from the sequence of quantum states associated with the sine-Gordon breather, where m is bounded by the coupling constant.[37,38] As indicated in Table VII, Eqs. (98) and (100) also apply to the AEH model by replacing D by $J(1-1/g)$.

The same quantum energy levels are obtained by using the quantization rule

$$M^z(\Omega)=m, \quad m=0,1,2,\ldots, \qquad (103)$$

that is to say, the spin deviation can adopt only integer values [Eqs. (7)–(9)]. From the soliton relations for M_z (Table VII), one then obtains $\Omega=\Omega(m)$. Substitution into the soliton energies yields $E=E(m)$, which turns out to be identical to Eq. (101), as obtained from the Bohr-Sommerfeld procedure.

In the IH case, where the classical oscillation frequency Ω has already been eliminated in the soliton energy, we may simply use Eq. (103), and for the momentum, the de Broglie rule

$$P=\hbar q \quad . \qquad (104)$$

TABLE VIII. Sequence of quantum states, obtained from the Bohr-Sommerfeld–de Broglie quantization of the classical soliton solution (Table VII). In the EAH and AEH models, the results correspond to the weak-coupling limit. EAH: $D/2JS \ll 1$ [Eq. (62)]; AEH: $g=2\epsilon^2+1$, $\epsilon^2 \ll 1$ [Eqs. (75) and (76)].

	$E(m)$
IH	$\frac{16}{m}Js^3\sin^2\frac{q}{4s}+hm$
EAH	$2mDs-\frac{1}{12}m^3\frac{D^2}{Js}$
AEH	$4Jms\epsilon^2\left(1-2\epsilon^2-\frac{m^2}{12s^2}\epsilon^2\right)$

The resulting quantum states are listed in Table VIII. In the AEH and EAH systems, weak coupling is assumed [Eqs. (62), (75), and (76)].

By comparing these results with the correct quantum expressions, it should be borne in mind that, in the systems considered here, the solitons are particular solutions only. In this view, it is really remarkable that in the IH case and $s=\frac{1}{2}$, the Bohr-Sommerfeld–de Broglie energies (Table VII) agree exactly with the full quantum results given in Table III, including the magnon. A numerical solution of the bound-state condition (56) indicates that the agreement extends for q small to general s values. This is obviously the case for $m=1$. In the EAH and AEH models, it is appropriate to compare with the quantum results, as obtained from the mapping on the Bose gas (Table V), valid in the continuum and weak-coupling limits. Comparing Tables V and VIII, it is seen that in both cases, agreement is obtained for large quantum numbers,

$$m^2 >> 1 \quad , \tag{105}$$

and for the EAH model for

$$s >> \tfrac{1}{2} \tag{106}$$

in addition. Nevertheless, also in these models, the success of the Bohr-Sommerfeld quantization is quite impressive if applied to the soliton solution, representing a bound kink-antikink pair. The restriction to large quantum numbers excludes, however, the magnon and the small m bound states.

ACKNOWLEDGMENTS

We have benefited from illuminating discussions with Ch. Enz, H. R. Jauslin, J. M. Loveluck, S. W. Lovesey, K. Maki, M. Steiner, and E. Stoll.

[1]See review articles on magnetic chains, in *Physics in One Dimension,* edited by J. Bernasconi and T. Schneider (Springer-Verlag, Heidelberg, 1981).
[2]M. E. Fisher, Am. J. Phys. 32, 343 (1964); H. Tomita and H. Mashyama, Prog. Theor. Phys. 48, 1133 (1972).
[3]J. M. Loveluck, S. W. Lovesey, and S. Aubry, J. Phys. C 8, 3841 (1975).
[4]M. V. Feigelman, Sov. Phys. Solid State 18, 1434 (1976) [Fiz. Tverd. Tela (Leningrad) 18, 2454 (1976)].
[5]K. Nakumara and T. Sasada, Solid State Commun. 21, 891 (1979).
[6]J. M. Loveluck, T. Schneider, E. Stoll, and H. R. Jauslin, Phys. Rev. Lett. 45, 1505 (1980).
[7]C. G. Windsor and J. Locke-Wheaton, J. Phys. C 9, 2749 (1976).
[8]P. Heller and M. Blume, Phys. Rev. Lett. 39, 962 (1977).
[9]G. Reiter and A. Sjölander, J. Phys. C 13, 3027 (1980).
[10]J. Tjon and J. Wright, Phys. Rev. B 15, 3470 (1977).
[11]A. E. Borovik and K. V. Maslov, Sov. J. Low Temp. Phys. 4, 47 (1978) [Fiz. Nizk. Temp. 4, 94 (1978)].
[12]L. A. Takhtajan, Phys. Lett. 64A, 235 (1977).
[13]E. K. Sklyanin (unpublished).
[14]H. A. Bethe, Z. Phys. 71, 205 (1931).
[15]R. J. Baxter, Ann. Phys. (N.Y.) 70, 193, 323 (1972).
[16]B. Sutherland, J. Math. Phys. (N.Y.) 17, 3183 (1970).
[17]J. D. Johnson, S. Krinsky, and B. M. McCoy, Phys. Rev. A 8, 2556 (1973).
[18]E. K. Sklyanin and L. D. Faddeev, Sov. Phys. Dokl. 23, 902 (1979) [Dok. Akad. Nauk SSSR 243, 7430 (1978)].
[19]P. P. Kulish and E. K. Sklyanin, Phys. Lett. 70A, 461 (1979).
[20]M. Wortis, Phys. Rev. 132, 85 (1963).
[21]J. Hanus, Phys. Rev. Lett. 11, 336 (1963).
[22]R. Orbach, Phys. Rev. 112, 309 (1958).
[23]I. G. Gochev, Sov. Phys. JETP 34, 892 (1972) [Zh. Eksp. Teor. Fiz. 61, 1674 (1971)].
[24]Ch. K. Majumdar, Phys. Rev. B 1, 287 (1970).
[25]J. B. Torrance, Jr., and M. Tinkham, Phys. Rev. 187, 595 (1969).
[26]R. Silberglitt and J. B. Torrance, Phys. Rev. B 2, 772 (1970).
[27]V. E. Zakharov and L. A. Takhtajan, Theor. Math. Phys. 38, 17 (1979).
[28]H. C. Fogedby, J. Phys. A 13, 1467 (1980).
[29]F. J. Dyson, Phys. Rev. 102, 1217, 1230 (1956).
[30]S. V. Maleev, Sov. Phys. JETP 6, 776 (1956) [Zh. Eksp. Teor. Fiz. 33, 1010 (1957)].
[31]S. W. Lovesey, *Condensed Matter Physics* (Benjamin, Reading, Mass., 1980).
[32]J. B. McGuire, J. Math. Phys. 5, 622 (1964).
[33]K. A. Long and A. R. Bishop, J. Phys. A 12, 1325 (1979).
[34]A. Jevicki and N. Papanicolau, Ann. Phys. (N.Y.) 120, 107 (1979).
[35]H. C. Fogedby (unpublished).
[36]A. Messiah, *Quantum Mechanics* (North-Holland, Amsterdam, 1965), Vol. I, p. 34.
[37]S. Coleman, in *New Phenomena in Subnuclear Physics,* edited by A. Zichichi (Plenum, New York, 1977).
[38]R. F. Dashen, B. Hasslacher, and A. Neveu, Phys. Rev. B 10, 4130 (1974).